Mathematical and Computer Modelling 57 (2013) 1350–1359

Contents lists available at SciVerse ScienceDirect

Mathematical and Computer Modelling

journal homepage: www.elsevier.com/locate/mcm

A fast algorithm for computing the flux around non-overlapping disks on the plane

Vladimir Mityushev [a,*], Natalia Rylko [b]

[a] Department of Computer Sciences and Computer Methods, Pedagogical University, ul. Podchorazych 2, Krakow 30-084, Poland

[b] Department of Technology, Pedagogical University, ul. Podchorazych 2, Krakow 30-084, Poland

ARTICLE INFO

Article history:
Received 16 November 2011
Received in revised form 26 October 2012
Accepted 6 November 2012

Keywords:
Method of images
Non-overlapping disks
Multiply connected domain

ABSTRACT

Conductivity of n non-overlapping disks embedded in a two-dimensional background can be investigated by the method of images which is based on the successive application of the inversions with respect to circles. For closely placed disks, the classical method of images yields slowly convergent series. The method of images can be treated as an application of successive approximations to a system of functional equations. In this paper, modified functional equations are deduced to essentially accelerate the convergence.

1. Introduction

The transport properties of unidirectional circular cylinders are of considerable interest in the electrical or thermal conductivity, the dielectric permittivity and other fields governed by the Laplace equation. This problem can be reduced to a two-dimensional problem for non-overlapping disks on the plane. Various methods were applied to calculate the local field and to estimate the macroscopic behavior of circular cylinders [1–7]. Majority of the previous analytical methods were related to the method of images [3,7], because this method is simple in calculations and yields analytical formulas important in applications.

The method of images for n non-overlapping disks on the plane is based on the successive application of the inversions with respect to circles. Each inversion transforms a harmonic function in the disk to a harmonic function out of the disk and vice versa. In the case $n \geq 2$, the inversions generate an infinite group of their compositions called the Schottky group. In order to solve a boundary value problem for the exterior of the disks one has to use infinite series involving all elements of the Schottky group. In the case $n = 2$, such series converge and can be presented in terms of the elliptic functions and sometimes even of the elementary functions. In the case $n \geq 3$, more complicated classes of functions arise. They can be presented in the form of the uniformly convergent Poincaré series [8]. Though such series theoretically converge for any multiply connected circular domain, practical computations can be very expensive because of their slow convergence.

McPhedran et al. [9–12] extended the method of Lord Rayleigh to calculate the effective conductivity of regular arrays. The method of functional equations was applied in [7] to estimate the effective conductivity for arbitrary locations of the disks.

Berlyand, Kolpakov and Novikov [13–15] proposed structural approximations based on the network approach to estimate the macroscopic properties of highly filled contrast composites. Rylko [16] compared the methods of functional equations, i.e., the method of images and structural approximations and showed that for closed disks a huge number of iterations are

* Corresponding author. Tel.: +48 12 6626276; fax: +48 12 6358858.
E-mail address: mityu@up.krakow.pl (V. Mityushev).

0895-7177/$ – see front matter
doi:10.1016/j.mcm.2012.11.019

needed for sufficiently precise estimation of the flux. It was also investigated for which sizes of gaps between the disks and for which their conductive properties structural approximations yield correct results.

Methods of integral equations were developed in [17,5,18] and others to numerically solve the considered problems. The fast multipole method was applied in [17] to solve the resulting integral equations. These methods are effective in numerical computations when the geometry of the problem is fixed.

Though many efforts were applied to investigate the multiple disk problem in analytical form, the existing methods do not give effective analytical formulas for the flux around densely packed non-overlapping disks.

In the present paper, we modify the method of functional equations to construct a fast algorithm to compute the flux around disks in analytical form. The main idea is based on reduction of the problem to a system of functional equations. The functional equations discussed in [8,7,16] were solved by successive approximations. Actually, the method of images was formulated in the form of iterative functional equations that makes it convenient in realization. Though, the uniform convergence of the approximations was proved and lower order formulas were deduced, the problem of the speed of convergence was opened. The main reason of the slow convergence is explained by two different scales of the given terms of equations and of its solution. In the present paper, functional equations are modified in such a way that the order of the given terms of equations coincides with the order of the solution. This resolves the convergence problem.

The case of three disks is considered in detail. It is shown that about 6 iterations are sufficient to obtain good approximations. The number of iterations was few hundreds in the classical method of images [16]. Thus, the method of images, simple in symbolic manipulations, becomes simple in computations.

2. Method of complex potentials

It is convenient to use the complex variable $z = x + iy$ on the complex plane $\mathbb{C}$. Consider non-overlapping disks $D_k = \{z \in \mathbb{C} : |z - a_k| < r_k\ (k = 1, 2, \dots, n)\}$. Let the boundary of D_k, the circle $|t - a_k| = r_k$, is oriented in the counter clockwise direction. Let D denote the complement of the closed disks $|z - a_k| \leq r_k$ to the extended complex plane $\mathbb{C} \cup \{\infty\}$.

Let the domain D be occupied by a conducting material. Consider the classical capacity problem when the potential $u(x, y) \equiv u(z)$ satisfies the Laplace equation $\Delta u = 0$ in D with the Dirichlet boundary conditions

$$u(t) = u_k, \qquad |t - a_k| = r_k, \quad k = 1, 2, \dots, n, \tag{2.1}$$

where u_k are given constants. We are looking for the potential $u(z)$ and the flux $\nabla u = (u_x, u_y)$. Here, u_x and u_y denote the partial derivatives of u on x and y, respectively.

Following [7] we reduce the problem (2.1) to a Riemann–Hilbert problem. First, consider the unit orthonormal vector $\mathbf{n} = (n_1, n_2)$ outward to the circle $|t - a_k| = r_k$ and the tangent vector $\mathbf{s} = (-n_2, n_1)$. Let $n(t) = \frac{1}{r_k}(t - a_k)$ and $s(t) = in(t)$ express these vectors in terms of complex values. Differentiate the boundary condition (2.1) on $\mathbf{s}$ as follows:

$$\frac{\partial u}{\partial \mathbf{s}} = -n_2 u_x + n_1 u_y = 0, \qquad |t - a_k| = r_k, \quad k = 1, 2, \dots, n. \tag{2.2}$$

Introduce the complex potential analytic in D

$$\psi(z) = u_x - iu_y \tag{2.3}$$

and rewrite (2.2) in the form

$$Im\, \frac{t - a_k}{r_k}\psi(t) = 0, \quad |t - a_k| = r_k, k = 1, 2, \dots, n. \tag{2.4}$$

This relation can be considered as a Riemann–Hilbert problem with respect to $\psi(z)$ analytic in D and continuous in its closure.

Let us assume that

$$|\psi(z)| = O(|z|^{-2}), \quad \text{as } z \to \infty. \tag{2.5}$$

It follows from [19] that the problem (2.4)–(2.5) has $(n - 1)$ $\mathbb{R}$-linear independent solutions. The structure of the general solution has the form

$$\psi(z) = \sum_{m=1}^{n} A_m \Psi^{(m)}(z), \tag{2.6}$$

where $(n - 1)$ functions $\Psi^{(m)}(z)$ (let it be $m = 1, 2, \dots, n - 1$) generate a set of fundamental solutions of (2.4) and real constant A_k satisfy the condition

$$\sum_{m=1}^{n} A_m = 0. \tag{2.7}$$

Let $\Phi^{(m)}(z)$ be a primitive function of $\Psi^{(m)}(z)$, i.e., $\frac{d}{dz}\Phi^{(m)}(z) = \Psi^{(m)}(z)$ in D. Then the indefinite integral of $\psi(z)$ has the form

$$\phi(z) = \sum_{m=1}^{n} A_m \Phi^{(m)}(z) + c_0, \tag{2.8}$$

where c_0 is an arbitrary constant. It follows from (2.2) and (2.4) that

$$\frac{\partial Re\phi}{\partial \mathbf{s}} = 0, \qquad |t - a_k| = r_k, \quad k = 1, 2, \ldots, n. \tag{2.9}$$

Therefore, $Re\phi(z)$ is constant on each circle $|t - a_k| = r_k$ for any choice of A_k and c_0. In particular, $\alpha_{km} = Re\ \Phi^{(m)}(z)$ are constant on $|t - a_k| = r_k$. Only one of all the functions (2.8) satisfies the boundary condition

$$Re\ \phi(t) = u_k, \qquad |t - a_k| = r_k, \quad k = 1, 2, \ldots, n, \tag{2.10}$$

where u_k are given constants in (2.1). The relation (2.10) yields the system of linear algebraic equations with respect to the real constants A_k $(k = 1, 2, \ldots, n)$ and $A_0 = Rec_0$

$$\sum_{m=0}^{n} \alpha_{km} A_m = u_k, \qquad |t - a_k| = r_k, \quad k = 0, 1, \ldots, n, \tag{2.11}$$

where $\alpha_{k0} = 1$ and $u_0 = 0$. The zeroth equation (2.11) $(k = 0)$ coincides with (2.7). This system always has a unique solution for any u_k since in the opposite case it contradicts to the existence of the unique solution of the Dirichlet problem (2.1).

3. $\mathbb{R}$-linear problem and functional equations

In the present section, the problem (2.4) is reduced to a system of functional equations via the $\mathbb{R}$-linear problem. It follows from [19] that the boundary value problem (2.4) is equivalent to the $\mathbb{R}$-linear problem

$$\psi(t) = \psi_k(t) + \left(\frac{r_k}{t - a_k}\right)^2 \overline{\psi_k(t)} + \frac{A_k}{t - a_k}, \quad |t - a_k| = r_k, k = 1, 2, \ldots, n, \tag{3.1}$$

where $\psi_k(z)$ is analytic in $|z - a_k| < r_k$ and continuous in $|z - a_k| \le r_k$. Here, the constants A_k are fixed. One can assume that these constants A_k are the same as in the representation (2.6). Fix m and denote the Kronecker symbol by δ_{mk}. Then putting $A_k = \delta_{mk}$ we arrive at the problem (3.1) with $\psi(z) = \Psi^{(m)}(z)$.

The problem (3.1) was reduced to the system of functional equations [19]

$$\psi_k(z) = \sum_{m \ne k} \left(\frac{r_m}{z - a_m}\right)^2 \overline{\psi_m\left(z^*_{(m)}\right)} + \sum_{m \ne k} \frac{A_m}{t - a_m}, \tag{3.2}$$

where

$$z^*_{(m)} = \frac{r_m^2}{\overline{z - a_m}} + a_m \tag{3.3}$$

denotes the inversion with respect to the circle $|t - a_m| = r_m$. Let $\psi_k(z)$ $(k = 1, 2, \ldots, n)$ be a solution of (3.2). Then

$$\psi(z) = \sum_{m=1}^{n} \left(\frac{r_m}{z - a_m}\right)^2 \overline{\psi_m\left(z^*_{(m)}\right)} + \sum_{m=1}^{n} \frac{A_m}{z - a_m}, \quad z \in D. \tag{3.4}$$

Lemma 3.1 *([8, Lemma 4.8, p. 167], [19]). The system (3.2) has a unique solution. This solution can be found by the method of successive approximations uniformly convergent in each disk $|z - a_k| \le r_k$.*

It is worth noting that from all known iterative schemes and infinite series (see references in Introduction and in [19]) only the system (3.2) can be solved by successive approximations for any location of non-overlapping disks including touching of the disks. Moreover, exact formulas in the form of series are written in [19].

Two iterative schemes were proposed to obtain approximate solutions in analytical form of the system (3.2) (for details see [20,21]). The first method is based on the direct iterations and actually coincides with a modified method of images. The second method is based on the expansion on $r = \max_{1 \le k \le n}\{r_k\}$. The second method gives new analytical exact and approximate formulas for the effective conductivity of composites. This method is also effective for the computation of the dipoles of the finite numbers of disks on the plane [16].

Though the theoretical problem of convergence was solved and new analytical formulas for the macroscopic properties were deduced in the above cited papers, the successive approximations converge slowly for densely placed disks. It was known to previous investigators and directly shown in [16] that application of the functional equations (3.2) is not effective for the computation of the local fields. The latter fact is related to the following observations. First, the series from [19] can be conditionally convergent. It is a typical situation for densely placed disks, since all known results of the absolutely convergent series include geometrical restrictions. Here, we present such a typical restriction expressed in terms of the separated parameter Δ introduced by Henrici and used by DeLillo et al. [22]

$$\Delta = \max_{k\neq m} \frac{r_k + r_m}{|a_k - a_m|} < \frac{1}{(n-1)^{\frac{1}{4}}}. \tag{3.5}$$

The latter inequality roughly means that each disk is sufficiently far away from others. It is well known that conditionally convergent series are slowly convergent. Second, the flux between two disks tends to infinity if the distance between the disks tends to zero [14–16]. So, this infinity should be obtained from bounded values of the linear equations (3.2) by additive operations. It is clear that such a number of operations should be huge to get an acceptable result.

4. Structural approximation and the two disk problem

In Section 5, new functional equations are deduced to overcome the problem of slow convergence described in the previous section. The form of the new equations and a theoretical justification of the fast convergence are based on the theory of structural approximation developed by Berlyand and Kolpakov [14,15] and extended in [13,16]. Below, we summarize these results.

Voronoi tessellations for the considered disks are defined as a set of points that are closer to the given disk than to the remaining ones. It is known that the Voronoi tessellation consists of the polygons. Let us fix a disk (i.e., fix a number m) lying in a polygon P_m of the Voronoi tessellation. Let the polygon P_m has the joint sides with other polygons P_k for some $k \in J_m$. The disks D_k ($k \in J_m$) are called neighboring to D_m. The graph with the edges connecting the neighboring nodes a_m ($m = 1, 2, \ldots, n$) is referred to as the Delaunay graph.

Introduce the ratio of the distance between two disks D_k and D_ℓ to the distance between their centers

$$\delta_{k\ell} = 1 - \frac{r_k + r_\ell}{|a_k - a_\ell|}. \tag{4.1}$$

The parameter $\delta = \min_{k\ell}\{\delta_{k\ell}\}$ plays an important role in the theory of structural approximation. It is related to the separation parameter (3.5) by formula $\delta = 1 - \Delta$.

The flux between the neighboring disks D_k and D_ℓ is of order (see formula (5.6) from [16])

$$\frac{|u_k - u_\ell|}{\delta_{k\ell}} + O(1), \quad \text{as } \delta_{k\ell} \to 0. \tag{4.2}$$

Therefore, it tends to infinity as $\delta_{k\ell}$ tends to zero. This observation justifies the remark from the previous section that the flux between disks can considerably exceed the bounded entries of the functional equations (3.2).

In order to modify Eqs. (3.2) consider an auxiliary problem with two disks. Let the domain G be the complement of two disjoint disks $|z - a_k| \leq r_k$ ($k = 1, 2$) to the extended complex plane. The quadratic equation $z^*_{(1)} = z^*_{(2)}$ with respect to z (see (3.3)) has two roots

$$\begin{aligned} z_{12} &= \frac{a_1 + a_2}{2} + \frac{r_1^2 - r_2^2}{2(\overline{a_2 - a_1})} - \frac{a_2 - a_1}{2}\sqrt{1 + \frac{(r_1^2 - r_2^2)^2}{4|a_2 - a_1|^4} - 2\frac{r_1^2 + r_2^2}{|a_2 - a_1|^2}} \in D_1, \\ z_{21} &= \frac{a_1 + a_2}{2} + \frac{r_1^2 - r_2^2}{2(\overline{a_2 - a_1})} + \frac{a_2 - a_1}{2}\sqrt{1 + \frac{(r_1^2 - r_2^2)^2}{4|a_2 - a_1|^4} - 2\frac{r_1^2 + r_2^2}{|a_2 - a_1|^2}} \in D_2. \end{aligned} \tag{4.3}$$

The complex potential

$$\Psi(z) = \frac{1}{z - z_{12}} - \frac{1}{z - z_{21}} \tag{4.4}$$

describes the flux between the disks when the difference $u_1 - u_2$ of the potentials on the boundaries of the disks is equal to

$$u_1 - u_2 = \ln \frac{1 - \sqrt{d}}{1 + \sqrt{d}}, \qquad d = \frac{|a_2 - a_1|^2 - (r_1 + r_2)^2}{|a_2 - a_1|^2 - (r_1 - r_2)^2}. \tag{4.5}$$

Formulas (4.3)–(4.5) generalize the corresponding formulas form [16] deduced for $r_1 = r_2$ (see also [23]).

5. Modified functional equations

Now, we are ready to introduce modified functional equations. The main idea is based on the decomposition of the complex flux $\psi(z)$ onto $\psi_\delta(z)$ and $\psi_0(z)$ where the given singular part $\psi_\delta(z)$ amounts to the functions

$$\Psi(z; m, \ell) = \frac{1}{z - z_{m\ell}} - \frac{1}{z - z_{\ell m}} \tag{5.1}$$

introduced similar to (4.4). The functions $\Psi(z; m, \ell)$ have the required order (4.2) in the necks between the disks. Hence, the boundary value problem with respect to $\psi_0(z)$ and the corresponding functional equations contain terms of the proper order. Thus, the known and unknown terms in such equations are in equilibrium that is important in computations.

First, the set of fundamental solutions $\Psi^{(m)}(z)$ $(m = 1, 2, \dots, n-1)$ in the representation (2.6) is chosen in the following way. Let m be fixed. Let the disks D_ℓ for $\ell \in J_m$ be neighboring for D_m. $\Psi^{(m)}(z)$ is determined from such a boundary value problem (deduced below as (5.4) or (5.5)) that the singular function $\psi_\delta(z)$ has the form

$$\psi_\delta^{(m)}(z) = \sum_{\ell \in J_m} \Psi(z; m, \ell). \tag{5.2}$$

The functions $\Psi^{(m)}(z)$ $(m = 1, 2, \dots, n)$ generate a complete set of fundamental solutions since each function $\Psi^{(m)}(z)$ dominates in the necks between D_m and D_ℓ $(\ell \in J_m)$.

For definiteness, we now proceed to deduce functional equations corresponding to a fixed fundamental solution $\Psi^{(m)}(z)$. Therefore, a special solution of the boundary value problem (2.4) is looked for in the form

$$\psi^{(m)}(z) = \psi_0^{(m)}(z) + \psi_\delta^{(m)}(z), \quad z \in D, \tag{5.3}$$

where $\psi_\delta^{(m)}(z)$ is given by (5.2). Hereafter, the superscript (m) is omitted for brevity. The boundary value problem (2.4) becomes

$$Im \frac{t - a_k}{r_k} [\psi_0(t) + \psi_\delta(t)] = 0, \quad |t - a_k| = r_k, k = 1, 2, \dots, n. \tag{5.4}$$

Introduce the function

$$f_k^{(m)}(z) = f_k(z) := \begin{cases} 0, & k = m, \\ \displaystyle\sum_{\ell \in J_m; \ell \neq k} \Psi(z; m, \ell)(z), & k \in J_m, \\ \displaystyle\sum_{\ell \in J_m} \Psi(z; m, \ell)(z), & k \in J_m^*, \end{cases}$$

where J_m^* is the complement of $J_m \cup \{m\}$ to $\{1, 2, \dots, n\}$. One can see that $f_k(z)$ is analytic in $|z - a_k| < r_k$. Using the properties of the function (5.1) established in the previous section one can check the relations

$$Im \frac{t - a_m}{r_m} \Psi(t; m, \ell) = 0, \quad |t - a_m| = r_m$$

and

$$Im \frac{t - a_\ell}{r_\ell} \Psi(t; m, \ell) = 0, \quad |t - a_\ell| = r_\ell.$$

Then (5.4) can be written in the form

$$Im \frac{t - a_k}{r_k} [\psi_0(t) + f_k(t)] = 0, \quad |t - a_k| = r_k, k = 1, 2, \dots, n. \tag{5.5}$$

The boundary value problem (5.5) is equivalent to the $\mathbb{R}$-linear problem

$$\psi_0(t) = \psi_k(t) + \left(\frac{r_k}{t - a_k}\right)^2 \overline{\psi_k(t)} - f_k(t) + \frac{r_k \alpha_k}{t - a_k}, \quad |t - a_k| = r_k, k = 1, 2, \dots, n, \tag{5.6}$$

where α_k are real constants. In order to prove this, first, rewrite the condition (5.6) in the form

$$\frac{t - a_k}{r_k} \psi_0(t) = \frac{t - a_k}{r_k} \psi_k(t) + \overline{\frac{t - a_k}{r_k}} \overline{\psi_k(t)} - \frac{t - a_k}{r_k} f_k(t) + \alpha_k, \quad |t - a_k| = r_k, k = 1, 2, \dots, n, \tag{5.7}$$

where the relation $\overline{\frac{t-a_k}{r_k}} = \frac{r_k}{t-a_k}$ on the circle $|t - a_k| = r_k$ is used. The imaginary part of (5.7) coincides with (5.5). Therefore, (5.7) implies (5.5).

Conversely, let $\psi_0(z)$ be a solution of (5.5). The function $\Psi_k(z) = \frac{\alpha_k}{2} + (z - a_k)\ \psi_k(z)$ can be uniquely determined from the simple Schwarz problem for the disk D_k [8]

$$2Re\ \Psi_k(t) = Re\frac{t - a_k}{r_k}[\psi_0(t) + f_k(t)], \quad |t - a_k| = r_k. \tag{5.8}$$

The latter problem has a unique solution, since $Im\Psi_k(a_k) = 0$. Therefore, the function $\psi_k(z)$ and the constant α_k are uniquely determined in terms of $\psi_0(z) + f_k(z)$ for each $k = 1, 2, \ldots, n$. By construction, $\psi_k(z)$ $(k = 0, 1, \ldots, n)$ satisfy (5.6).

Each set of constants α_k $(k = 1, 2, \ldots, n)$ determines the corresponding function $\psi_0(z)$ via the solution to the problem (5.6). One can see that the function (5.3) will not be identically zero if we put all $\alpha_k = 0$. This function will be taken as the fundamental solution $\Psi^{(m)}(z)$. Changing m, i.e., changing the functions $\psi_\delta^{(m)}(z) = \psi_\delta(z)$ we obtain another fundamental solution, because of the different behavior near the boundaries of the disks.

The $\mathbb{R}$-linear problem (5.6) (with $\alpha_k = 0$) can be reduced to functional equations. Following [19,8] introduce the function

$$\Phi(z) := \begin{cases} \psi_k(z) - \sum\limits_{m\neq k} \left(\dfrac{r_m}{z - a_m}\right)^2 \overline{\psi_m\left(z^*_{(m)}\right)} - f_k(z), |z - a_k| \leq r_k, & k = 1, 2, \ldots, n, \\ \psi_0(z) - \sum\limits_{m=1}^{n} \left(\dfrac{r_m}{z - a_m}\right)^2 \overline{\psi_m\left(z^*_{(m)}\right)}, & z \in D \end{cases}$$

analytic in the domains $D_k (k = 1, 2, \ldots, n)$ and D. Calculate the jump across the circle $|t - a_k| = r_k$

$$\Delta_k := \Phi^+(t) - \Phi^-(t), \qquad |t - a_k| = r_k,$$

where $\Phi^+(t) := \lim_{z\to t\ z\in D} \Phi(z)$, $\Phi^-(t) := \lim_{z\to t\ z\in D_k} \Phi(z)$. Using (5.6) we get $\Delta_k = 0$. It follows from the Analytic Continuation Principle that $\Phi(z)$ is analytic in the extended complex plane. Moreover, $\psi_0(\infty) = 0$ yields $\Phi(\infty) = 0$. Then Liouville's theorem implies that $\Phi(z) \equiv 0$. The definition of $\Phi(z)$ in $|z - a_k| \leq r_k$ yields the following system of functional equations

$$\psi_k(z) = \sum_{\ell\neq k} \left(\frac{r_\ell}{z - a_\ell}\right)^2 \overline{\psi_\ell\left(z^*_{(\ell)}\right)} + f_k(z). \tag{5.9}$$

Lemma 3.1 holds for the functional equations (5.9). Hence, the following algorithm can be applied

$$\psi_k^{(0)}(z) = f_k(z), \tag{5.10}$$

$$\psi_k^{(p)}(z) = \sum_{m\neq k} \left(\frac{r_\ell}{z - a_\ell}\right)^2 \overline{\psi_\ell^{(p-1)}\left(z^*_{(\ell)}\right)} + f_k(z), \quad p = 1, 2, \ldots. \tag{5.11}$$

The p-th approximation of the complex flux is calculated by formula

$$\psi^{(p)}(z) = \sum_{\ell=1}^{n} \left(\frac{r_\ell}{z - a_\ell}\right)^2 \overline{\psi_m^{(p)}\left(z^*_{(\ell)}\right)} + \psi_\delta(z), \quad z \in D, \tag{5.12}$$

where $\psi_\delta(z)$ is given by (5.2).

6. Example. Three disks

Consider three disks $(n = 3)$ with the centers at the points $a_1 = \frac{1}{\sqrt{3}}$, $a_2 = \frac{1}{\sqrt{3}}\ e^{\frac{2}{3}\pi i}$, $a_3 = \frac{1}{\sqrt{3}}\ e^{-\frac{2}{3}\pi i}$. Below, these centers are fixed and radii vary.

Fundamental functions can be computed by the following two methods. First, consider the slow method based on the functional equations (3.2) with the above given data. Put $m = 1$ and $A_1 = 1, A_2 = A_3 = -\frac{1}{2}$. Then Eqs. (3.2) have a unique solution and the corresponding fundamental function is calculated by (3.4). The functional equations (3.2) are solved by successive approximations. Hence, the fundamental function is represented in the form of a series. This series corresponds to the classical method of images. One can expect that this series slowly converges for small parameters (4.1).

Application of the modified functional equations (5.9) yields a fundamental function $\Psi^{(1)}(z)$. The function $f_k(z)$ becomes

$$f_k(z) = \begin{cases} 0 & \text{for } k = 1 \\ \dfrac{1}{z - z_{12}} - \dfrac{1}{z - z_{21}} & \text{for } k = 2 \\ \dfrac{1}{z - z_{13}} - \dfrac{1}{z - z_{31}} & \text{for } k = 3. \end{cases} \tag{6.1}$$

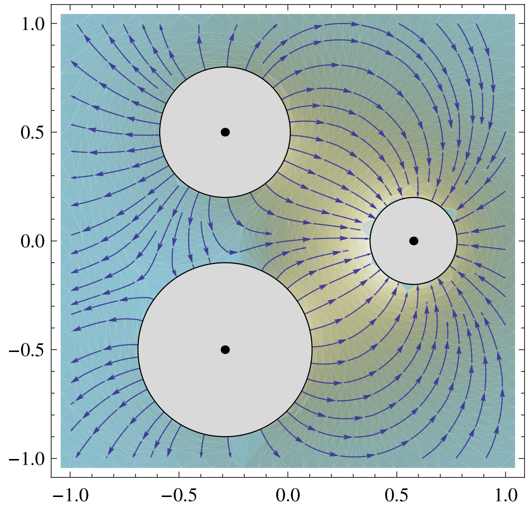

Fig. 1. Streamlines of the flux computed in the third order approximation around three disks with the centers at $a_1 = \frac{1}{\sqrt{3}}, a_2 = \frac{1}{\sqrt{3}} e^{\frac{2}{3}\pi i}, a_3 = \frac{1}{\sqrt{3}} e^{-\frac{2}{3}\pi i}$ of the radii $r_1 = 0.2, r_2 = 0.3, r_3 = 0.4$. Streamlines are directed in accordance with increasing potential. The higher intensity of the flux corresponds to more lighter areas.

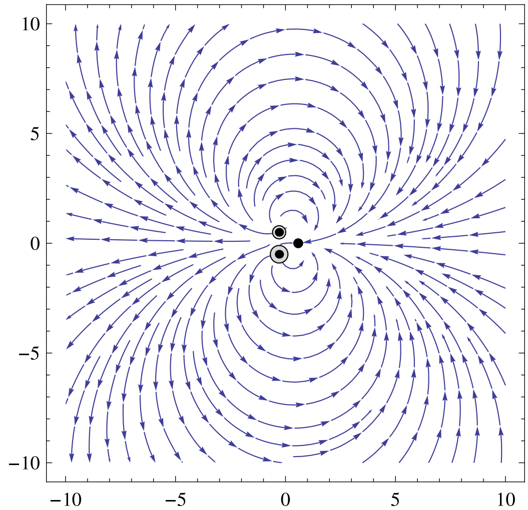

Fig. 2. Streamlines around the disks displayed in Fig. 1 in large domain where three disks are equivalent to a dipole in macroscale.

It is not necessary that $\Psi^{(1)}(z)$ coincides with the fundamental function obtained by Eqs. (3.2). This is not important because any flux between the disks charged by constant potentials can be obtained as a linear combination (2.6). Here, we are interested in the speed of convergence in both the methods.

The algorithm (5.10)–(5.12) yields approximate formulas for the complex flux for any geometrical parameters. One can substitute the data in (5.10)–(5.12) and obtain formulas in analytical form. Below we present the results obtained by this method. We use formulas (5.10)–(5.12) in general form and substitute the data in the final approximation $\psi^{(p)}(z)$. The order of approximation p is chosen by checking boundary conditions for $\frac{d}{dz}\Phi^{(1)}(z) = \Psi^{(1)}(z)$, namely, the function $Re\Phi^{(1)}(z)$ has to be constant on each circle (see (2.10)). Symbolic computations were performed in Mathematica©. It is interesting that it is practically impossible to look at the final long formulas, but one can easily compute values at given points, draw various plots and perform other operators of Mathematica©(length, coefficients, poles, series approximations etc.).

Figs. 1–3 describe the flux around three well-separated disks. In order to check the criterion of convergence the values of the potential on the circles are computed. They must be constants on circles. As it follows from Table 1 the potential $Re\Phi^{(1)}(z)$ is equal to 2.82, −1.12, −0.85 on the circles with the numbers 1, 2, 3, respectively. It is observed on Tables 1–3 that the modified equations (5.9) yield much better results than Eqs. (3.2) corresponding to the classical method of images. Note that this is the case of well-separated disks.

Fig. 4 describes the flux around three closely placed disks of radius 0.49. The potential on the disks is presented in Table 4. The flux in the thin neck between the first and second disks is given in Table 5. It follows from computations that 6 iterations

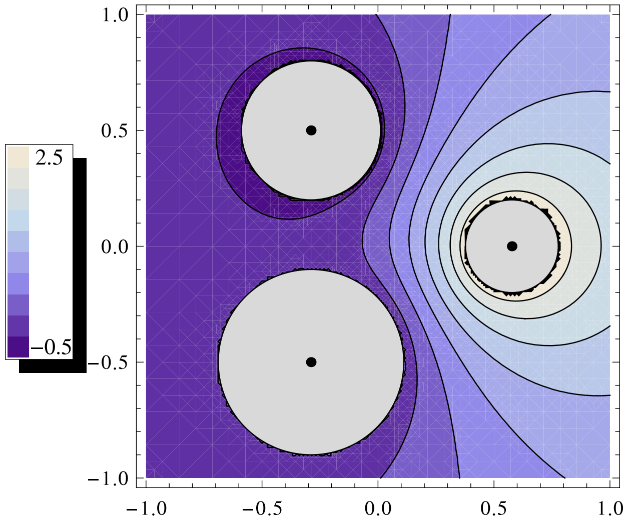

Fig. 3. Level contours of the potential $Re\Phi^{(1)}(z)$ around the disks displayed in Fig. 1.

Table 1
Potential $Re\Phi^{(1)}(a_1 + 0.2e^{i\theta})$ on the first circle for the disks displayed in Fig. 1. It is computed by the modified method based on (5.9) for $p = 1, 2, 3$ iterations. The fifth column presents the results obtained by the third iteration of the classical method of images based on (3.2).

θ	$p = 1$	$p = 2$	$p = 3$	Classical
−3	2.80898	2.82366	2.82145	2.95511
−2	2.78190	2.82456	2.82069	3.07032
−1	2.79915	2.82388	2.82116	3.23250
0	2.81706	2.82371	2.82172	3.29772
1	2.82451	2.82460	2.82205	3.23192
2	2.82493	2.82541	2.82214	3.06929
3	2.81828	2.82375	2.82176	2.95487

Table 2
Potential $Re\Phi^{(1)}(a_2 + 0.3e^{i\theta})$ on the second circle for the disks displayed in Fig. 1. Conventions are the same as in Table 1.

θ	$p = 1$	$p = 2$	$p = 3$	Classical
−3	−1.07535	−1.12454	−1.11768	−1.64441
−2	−1.02991	−1.12975	−1.11613	−1.71314
−1	−1.11320	−1.12088	−1.11887	−1.11679
0	−1.15974	−1.11793	−1.12028	−0.67196
1	−1.14903	−1.11834	−1.11995	−0.97842
2	−1.12512	−1.11990	−1.11923	−1.32326
3	−1.08896	−1.12315	−1.11811	−1.58558

Table 3
Potential $Re\Phi^{(1)}(a_3 + 0.4e^{i\theta})$ on the third circle for the disks displayed in Fig. 1. Conventions are the same as in Table 1.

θ	$p = 1$	$p = 2$	$p = 3$	Classical
−3	−0.82702	−0.85019	−0.84566	−1.35627
−2	−0.84727	−0.84473	−0.84608	−1.03451
−1	−0.84056	−0.84057	−0.84633	−0.60122
0	−0.83686	−0.83686	−0.84648	−0.08601
1	−0.845181	−0.84518	−0.84605	−0.69385
2	−0.86235	−0.86235	−0.84457	−1.60714
3	−0.85238	−0.85238	−0.84548	−1.43608

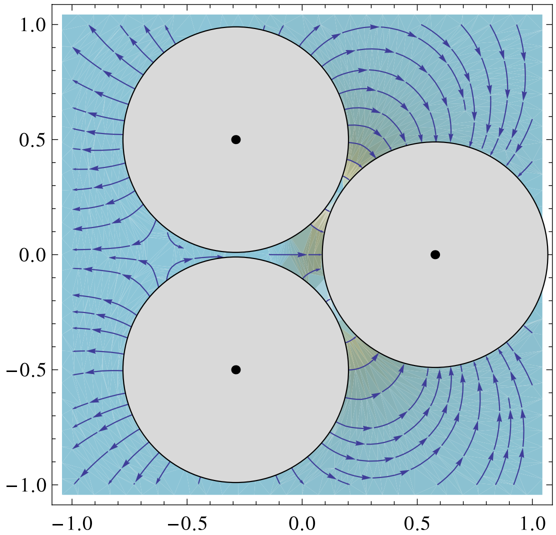

Fig. 4. Streamlines of the flux computed in the sixth order approximation around three disks with the centers at $a_1 = \frac{1}{\sqrt{3}}, a_2 = \frac{1}{\sqrt{3}} e^{\frac{2}{3}\pi i}, a_3 = \frac{1}{\sqrt{3}} e^{-\frac{2}{3}\pi i}$ of the radius 0.49.

Table 4
Potential $Re\Phi^{(1)}(a_3 + 0.49e^{i\theta})$ on the third circle for the disks displayed in Fig. 4. The "classical" column is the result of the sixth order iteration. Conventions are the same as in Table 1.

θ	$p = 4$	$p = 5$	$p = 6$	Classical
−3	−0.82702	−0.85019	−0.84566	−1.35578
−2	−0.84727	−0.84473	−0.84608	−1.03438
−1	−0.84056	−0.84057	−0.84633	−0.60140
0	−0.83686	−0.83686	−0.84648	0.08666
1	−0.845181	−0.84518	−0.84605	−0.69489
2	−0.86235	−0.86235	−0.84457	−1.60638
3	−0.85238	−0.85238	−0.84548	−1.43547

Table 5
Complex flux $\overline{\Psi^{(1)}(z)}$ in the neck between the first and second disks displayed in Fig. 4. Points in the first column are located between the disks on the line connecting the centers a_1 and a_2.

z	$p = 5$	$p = 6$
$0.153 + 0.245i$	$19.4812 - 11.3038i$	$19.6075 - 11.3058i$
$0.150 + 0.247i$	$19.3822 - 11.2398i$	$19.4963 - 11.2374i$
$0.147 + 0.248i$	$19.3266 - 11.2011i$	$19.4293 - 11.1945i$
$0.144 + 0.250i$	$19.3136 - 11.1872i$	$19.4056 - 11.1766i$
$0.141 + 0.251i$	$19.3431 - 11.1979i$	$19.4249 - 11.1834i$
$0.139 + 0.253i$	$19.4154 - 11.2333i$	$19.4874 - 11.2150i$
$0.136 + 0.255i$	$19.5315 - 11.294i$	$19.5941 - 11.2719i$

are sufficient to obtain an accessible result (see the criterion of constant potential verified on the third circle in Table 4). It is impossible to achieve such a precision by the classical method of images using 70 iterations. We suggest that few hundreds of iterations are also not sufficient [16].

7. Discussion

The method of images for n non-overlapping disks on the plane is equivalent to the method of successive approximations applied to functional equations (3.2). Slow convergence of the method of images can be explained by the following observations. Write Eqs. (3.2) for closely placed disks in the short form

$$x = Lx + f, \tag{7.1}$$

where x denote $\psi_k(z)$ in all the disks, L the linear operator on the right hand part of (3.2), f given functions with fixed A_k. It is worth noting that the constants A_k are proportional to the differences of the potentials on the circles and do not related to the intensity of the flux related to the geometrical gap parameter δ. Eq. (7.1) is considered in the Banach space of functions $x(z)$ analytic in the sum of disks $\cup_{k=0}^{n} D_k$ and continuous in their closures endowed with the norm $\|x\| = \max_{1\leq k\leq n} \max_{|z-a_k|\leq r_k} |x(z)|$ [8]. Convergence in this space means uniform convergence. The unique solution of (7.1) is presented in the form of the uniformly convergent series

$$x_0 = \sum_{k=0}^{\infty} L^k f. \tag{7.2}$$

Slow convergence of (7.2) for closely placed disks is explained by two different scales of f and x. The value f and the norm of the operator L are of order 1 but x_0 tends to infinity as $\delta \to 0$. It is clear that the sum (7.2) should contain many terms to achieve the true values. Here, the principle that the order of the zeroth approximation has to coincide with the order of the solution does not hold.

The modified method of functional equations involves the decomposition $x = x_\delta + x_0$ onto the singular part x_δ and the regular part x_0. The singular part x_δ is exactly written by (5.1)–(5.2). Then, (7.1) becomes

$$x_0 = Lx_0 + (Lx_\delta - x_\delta + f). \tag{7.3}$$

In this equation, x_0 and $Lx_\delta - x_\delta + f$ have the same bounded order. This explains fast convergence of the successive approximations for the modified functional equations (5.9).

Examples presented in Section 6 for three disks show advantages of the modified functional equations. Theory presented in Section 5 demonstrates that such effectiveness of the method is expected for many disks. Implementation of the method could be made by use of algorithms for Voronoi tessellation [13–15].

Acknowledgments

The authors are grateful to Professor Alexander A. Kolpakov and Professor M.V. Entov for stimulating discussions on the considered problems (with Vladimir Markovich in 2002). The first author is also grateful to Professor Ross McPhedran who paid attention to the three disk computational problem during fruitful discussions in 1999.

References

[1] I.V. Andrianov, V.V. Danishevskyy, D. Weichert, Simple estimations on effective transport properties of a random composite material with cylindrical fibres, ZAMP 2 (2008) 889–903.
[2] V.I. Bolshakov, I.V. Andrianov, V.V. Danishevskyy, Asymptotic Methods for Calculation of Composite Materials with Microstructure, Porogi, Dnipropetrovs'k, 2008 (in Russian).
[3] A.L. Kalamkarov, I.V. Andrianov, V.V. Danishevskyy, Asymptotic homogenization of composite materials and structures, Appl. Mech. Rev. 62 (2009) 030802-1–030802-20.
[4] D.G. Crowdy, The Schottky–Klein prime function on the Schottky double of planar domains, Comp. Meth. Funct. Theory 10 (2010) 501–517.
[5] E.I. Grigolyuk, L.A. Fil'shtinskij, Perforated Plates and Shells, Nauka, Moscow, 1970 (in Russian).
[6] G.W. Milton, The Theory of Composites, Cambridge University Press, 2002.
[7] V.V. Mityushev, E. Pesetskaya, S.V. Rogosin, Analytical methods for heat conduction in composites and porous media, in: A. Öchsner, G.E. Murch, M.J.S. de Lemos (Eds.), Cellular and Porous Materials: Thermal Properties Simulation and Prediction, Wiley, 2008, pp. 121–164.
[8] V.V. Mityushev, S.V. Rogosin, Constructive Methods for Linear and Non-Linear Boundary Value Problems for Analytic Function, Theory and Applications, Chapman & Hall/CRC, Boca Raton etc., 2000.
[9] R.C. McPhedran, Transport properties of cylinder pairs and of the square array of cylinders, Proc. R. Soc. Lond. A 408 (1986) 31–43.
[10] R.C. McPhedran, G.W. Milton, Transport properties of touching cylinder pairs and of the square array of touching cylinders, Proc. R. Soc. Lond. A 411 (1987) 313–326.
[11] R.C. McPhedran, L. Poladian, G.W. Milton, Asymptotic studies of closely spaced, highly conducting cylinders, Proc. R. Soc. Lond. A 415 (1988) 185–196.
[12] W.T. Perrins, D.R. McKenzie, R.C. McPhedran, Transport properties of regular arrays of cylinders, Proc. R. Soc. Lond. Ser. A 369 (1979) 207–225.
[13] L. Berlyand, A.G. Kolpakov, A. Novikov, Introduction to the Network Approximation, Method for Materials Modeling, in: Encyclopedia of Mathematics and Its Applications, vol. 148, Cambridge University Press, 2012.
[14] L. Berlyand, A. Kolpakov, Network approximation in the limit of small interparticle distance for the effective properties of high contrast random dispersed composites, Arch. Ration. Mech. Anal. 159 (2001) 179–227.
[15] A.A. Kolpakov, A.G. Kolpakov, Capacity and Transport in Contrast Composite Structures: Asymptotic Analysis and Applications, CRC Press Inc., Boca Raton etc., 2009.
[16] N. Rylko, Structure of the scalar field around unidirectional circular cylinders, Proc. R. Soc. A 464 (2008) 391–407.
[17] H. Cheng, L. Greengard, A method of images for the evaluation of electrostatic fields in systems of closely spaced conducting cylinders, SIAM J. Appl. Math. 58 (1998) 122–141.
[18] S.G. Mikhlin, Integral Equations and Their Applications to Certain Problems in Mechanics, Mathematical Physics and Technology, second rev. ed., Macmillan, NY, 1964.
[19] V.V. Mityushev, Riemann–Hilbert problems for multiply connected domains and circular slit maps, Comp. Meth. Funct. Theory 11 (2011) 575–590.
[20] V. Mityushev, Transport properties of doubly periodic arrays of circular cylinders and optimal design problems, Appl. Math. Optim. 44 (2001) 17–31.
[21] L. Berlyand, V. Mityushev, Increase and decrease of the effective conductivity of a two phase composites due to polydispersity, J Stat. Phys. 118 (2005) 481–509.
[22] T.K. DeLillo, T.A. Driscoll, A.R. Elcrat, J.A. Pfaltzgraff, Radial and circular slit maps of unbounded multiply connected circle domains, Proc. R. Soc. Lond. A 464 (2008) 1719–1737.
[23] L.D. Landau, E.M. Lifshitz, L.P. Pitaevskii, Electrodynamics of Continuous Media, Nauka, Moscow, 1982 (in Russian).